Studying Target Erosion in Sputtering Magnetrons Using a Discrete Numerical Model

C. Feist*, A. Plankensteiner**, C. Linke**, T. Kuniya***, J. Winkler**

* CENUMERICS, 6020 Innsbruck, Austria

** PLANSEE SE, 6600 Reutte, Austria

*** PLANSEE Japan Ltd., 107-0052 Tokyo, Japan

Abstract

Direct current (DC) discharges are widely used for sputtering of metals such as molybdenum or tungsten and formation of respective thin films on various types of substrates. Sputtering rate and deposition quality are increased by enhancing the discharge employing a static magnetic field such as within planar magnetrons. As a drawback and consequence of the distribution of the magnetic field target erosion becomes significantly non-uniform and overall target utilization is usually low.

Within the present work an implementation of a numerical model allowing to predict target erosion by means of resolving the distribution of ionization collisions and ion bombardment is shown. The model taken from literature is formulated in spirit of discrete models portraying the trajectories of energetic electrons in the discharge using a *Monte Carlo* approach. Using cross-sections formulated in terms of kinetic energy, collisions and scattering of electrons are modeled in a discrete fashion at random time-instants.

Furthermore, the model is modified by accounting for the collisions in a "smeared" rather than in discrete fashion by introducing a frictional force acting on the electrons still concisely accounting for the cross-sections of the considered collisions. Application of both the discrete and modified model is shown by means of a benchmark example from literature, thus, founding the theoretical basis for intended future optimizations of target erosion in DC magnetron sputtering applications.

Keywords

Sputtering, magnetron, target, erosion, numerical, model, simulation

Introduction

Sputtering processes allow formation of thin film depositions on various types of substrates by continuously eroding material such as molybdenum or tungsten from a target through ion bombardment.

The latter is usually established by a direct current (DC) discharge [1] between two electrodes placed within a reactor operated at the required pressure and supplied by an operating gas such as the noble gas argon (Ar) (Fig. 1). The target is bonded onto the cathode subjected to a stationary negative electric bias, whereas the anode usually carrying the substrate is grounded.

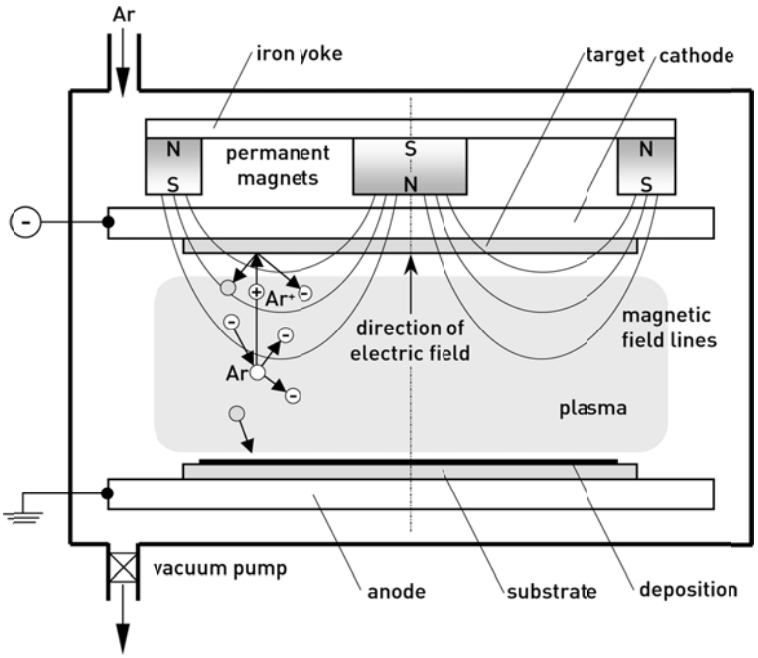

Figure 1: Schematic of a planar DC sputtering magnetron [1].

In contrast to other types of discharges such as inductive, radio frequency (RF) or microwave discharges, the plasma within a DC discharge is solely sustained by the flux of secondary electrons emitted from the target material upon bombardment by the positive gas ions [1], such as Ar^+ (Fig. 1). Hence, the latter is responsible both for sputtering and continuously sustaining the discharge along with the cathode bias. The electrons emitted from the target are accelerated by the electric field **E** found between the electrodes through the sheath into the plasma region to an energy level high enough to allow for ionizations of the operating gas. The created positive ions in turn are accelerated through the electric field towards the cathode where they sputter target atoms and trigger secondary electron emission (Fig. 1) with a certain probability. Ionization requires a certain level of kinetic energy of the impinging electron, which imposes certain restrictions onto the voltage applied to the cathode.

With the mean free path of the electrons usually of approximately the same order of magnitude as the reactor size electrons have to be confined to the region between the electrodes in order to increase the number of ionizations per electron and consequently the sputtering rate. Furthermore, electron confinement allows to operate the process at lower pressure reducing spurious (re-)depositions on the cathode or reactor walls and increasing sputtering quality [1]. The most usual type of confinement is provided through a static (also termed DC) magnetic field established by an array of permanent magnets arranged at the back of the cathode (Fig. 1). Within these so called magnetrons the interaction of the electric field and magnetic field – usually expressed in terms of the magnetic flux density **B** – at least confines those electrons emitted from a certain region of the cathode by forcing them to perform a more or less helical trajectory over the cathode with a drift along the **E** x **B** direction [1], i.e. the direction normal to the electric and magnetic field. This way, the drift direction becomes a geometric design

parameter for the layout of the electrodes, target and permanent magnet array with axisymmetric and rectangular designs with curved end sections being most common.

Depending on the shape of the confinement zone target erosion becomes non-uniform in the plane normal to the drift direction due to inhomogeneous density distribution of electrons able to perform ionization and consequently inhomogeneous distribution of ion bombardment. This is seen by the characteristic erosion profiles in sections normal to the drift direction and the characteristic racetracks found along the latter [2]. On the other hand, inevitable varying magnetic field intensities along the mean drift direction may lead to undesired *cross corner effects* occurring due to irregular drift velocity distribution and ionization probability at the curved end sections of rectangular targets [2].

Thus, as a drawback, target material is only utilized to a certain degree and non-uniform target erosion becomes a limiting factor. In view of this, various attempts have been made in the past to understand and study the mechanisms taking place in magnetically enhanced DC discharges and to improve the design of magnetrons in order to increase target utilization and lifetime. Such attempts are found both in the experimental and theoretical field by means of appropriate models and their analytical or numerical solution. On the other hand, modeling of discharges also allows to investigate effects and measure quantities not directly accessible or measurable by means of experiments.

The present work is motivated by efforts to improve lifetime of rectangular molybdenum targets used within planar magnetrons similar to the one depicted in Fig. 1. To this end, a numerical model of a magnetically enhanced DC discharge is developed, which should allow to predict the flux of bombarding ions which in turn can be used as a proxy for predicting the sputtering rate and consequently target erosion [3]. Application of the model should then allow for optimization of the magnetron with respect to increased target lifetime by controlling the magnetic field.

Numerical Methods for Plasma Modeling

Commonly discharges and plasmas are modeled based on either a (i) discrete, (ii) kinetic, or (iii) fluid-type description [4] with various hybrid forms of these basic classes. Discrete and kinetic approaches describe the plasma on a microscopic scale in terms of individual charged particles, i.e. electrons and ions, subjected to the *Lorentz* forces arising from the electromagnetic fields and inter-particle collisions. Kinetic approaches such as the *particle in cell* (PIC) method are usually based on a self-consistent plasma description with the charge density arising from electron and ion densities governing the underlying electric field which in turn determines the forces acting on the charged particles. In contrast, discrete approaches – usually implemented by means of *Monte Carlo* (MC) codes – try to trace a representative set of charged particles released in stochastic fashion and subjected to electromagnetic forces from reasonably assumed and imposed rather than self-consistently determined fields.

On the other hand, fluid-type models describe the plasma on a meso-scale based on the *Boltzmann*'s equation. With the latter being a complicated integro-differential equation in the six-dimensional phase space (in terms of particle velocities and positions) significant simplifications such as the two-term approximation [1] need to be made to solve for it. This allows to describe the plasma as a fluid defined in terms of electron density and mean electron density fields using meso-type constitutive properties (diffusivity and mobility) derived from an underlying electron energy distribution function (EEDF) [1, 4]. Fluid-type descriptions are usually based on finite element (FEM) or finite volume methods and allow to

account for a fully self-consistent description. In order to resolve the commonly observed steep gradients of the fields rather fine discretizations by elements or cells, respectively, are required rendering solutions for three-dimensional problems computationally quite expensive. In addition, for magnetically enhanced discharges constitutive properties become anisotropic with the magnetic cross-field diffusivity governed by the magnetic flux density [4]. With the latter differing from the streamline diffusivity by several orders of magnitude, numerical stability may be become negatively affected.

In view of these drawbacks, discrete plasma descriptions are still very attractive to use and besides allow for a rather intuitive interpretation of results in a classical mechanics framework.

Discrete Model for Trajectories of Energetic Electrons Undergoing Collisions With Neutrals

The model developed and implemented in the present work is based on such a discrete approach in spirit of the classical work of *Sheridan* and coworkers [3]. Without loss of generality the model is presented by considering an idealized representation of the axisymmetric planar magnetron studied by the same authors [5] as depicted in Fig. 2 (for simplicity shown upside down as compared to Fig. 1). The latter consists of a copper cathode of app. 108 mm in diameter serving also as a target placed above an array of permanent magnets coaxially arranged around a central cylindrical permanent magnet. The central magnet and the outer magnet array are connected using an iron pole plate. Argon (Ar) is used as background gas.

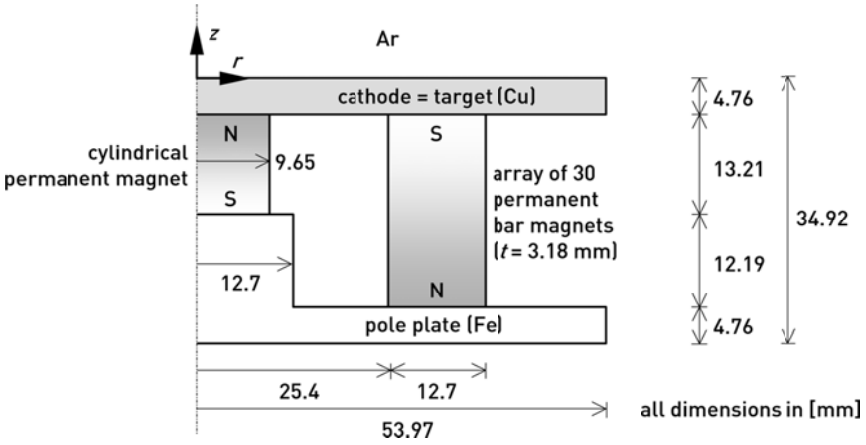

Figure 2: Sketch of the axisymmetric planar magnetron studied by [3, 5] and used as a benchmark for the present work.

Electromagnetic Fields

For the described discrete model weak coupling between the electromagnetic fields **E** and **B** and the motion of charged particles is considered. Hence, these fields are assumed or solved for independently of the orbits of charged particles but are used to drive the latter.

The electric field $\mathbf{E} = E\cdot\hat{z} = -\mathrm{d}\Phi/\mathrm{d}z$ is assumed to act along the axial direction $z \geq 0$, i.e. in direction normal to and above the target surface. The plasma is considered to be neutral in an average sense with equal number density of electrons n_e and ions n_i, i.e. $n_e = n_i = n_0$, and separated from the cathode surface by a sheath. The potential $\Phi(z)$ across the sheath is described in analytical fashion by means of a modification of the classical *Child's* law as proposed in [6]. The sheath is assumed to be connected to

a presheath within the plasma characterized by a constant electric field accelerating positively charged ions into the sheath. The potential drop across the presheath is usually negligible as compared to the one across the sheath. The model is described in non-dimensional fashion [6] using the cathode bias Φ_w, the approximate number density n_0, the *Mach* number *Ma*, and an estimate for the potential drop in the presheath as its parameters. For the present case a cathode bias of Φ_w = -400 V, a value quite common for magnetron DC discharges [1], is assumed according to [3]. The electron and ion number density, respectively, in the plasma are assumed as $n_0 = 2 \cdot 10^{10}$ cm^{-3} resulting in a *Debye* length and sheath thickness of app. 0.1 mm and 2.9 mm, respectively.

The neutral number density N in the reactor can be estimated using the ideal gas law $N = p/(k \cdot T)$ with k denoting the *Boltzmann* constant. At room temperature (T = 293.15 K) and a pressure of p = 1 Pa (≈ 7.5 mTorr) this yields $N \approx 2.47 \cdot 10^{14}$ cm^{-3} and an ionization degree typical for weakly ionized plasmas of $n_i / N \approx 8 \cdot 10^{-5}$.

With respect to the magnetic field **H** and the magnetic flux density **B** axisymmetric fields with vanishing azimuthal components $H_\varphi = B_\varphi = 0$ are assumed. Hence, the static magnetic field can be solved for by means of the finite element method using a two-dimensional model within the *rz*-plane (Fig. 3a). The nominal remanence of the permanent magnets is calibrated in order to obtain a flux density magnitude of 245 G at r = 17 mm on the cathode surface (Fig. 3b) comparable to the values reported in [3] and [5]. For the array of outer permanent magnets the remanence is reduced according to the solid fraction accounting for the gaps between the individual bar magnets. From the shape of the magnetic field lines shown in Fig. 3a and the magnetic flux density distribution over the cathode surface in Fig. 3b it can be seen that at $r \approx 19$ mm the magnetic field becomes parallel ($B_z = 0$) to the cathode surface which is empirically known to be the location of maximum erosion [2].

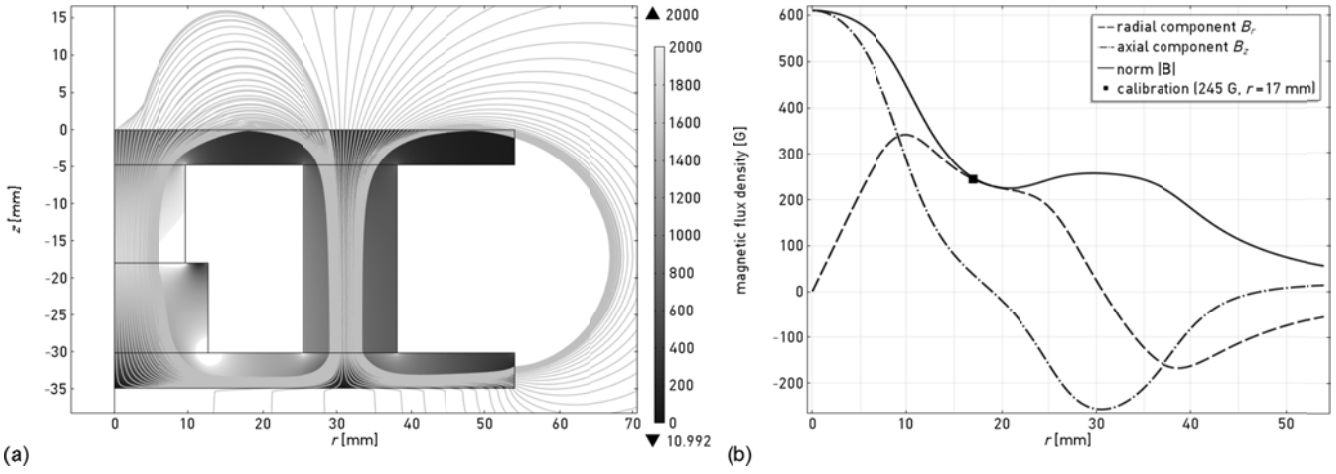

Figure 3: Computed static magnetic field: (a) contours of magnetic flux density norm (in G) and magnetic field lines (at equidistant distribution over cathode surface), (b) magnetic flux density distribution over cathode surface z = 0.

Equation of Motion of Charged Particles

A charged particle of mass m and charge q is subjected to the *Lorentz* forces from the electric field **E** and the magnetic flux density **B** expressed by the equation of motion

$$\mathbf{a} = q/m \cdot (\mathbf{E} + \mathbf{v} \times \mathbf{B}) \qquad (1)$$

with $\mathbf{a} = d^2\mathbf{x}/dt^2$ and $\mathbf{v} = d\mathbf{x}/dt$ as the particle acceleration and velocity vector, respectively. For given electric and magnetic fields the position $\mathbf{x}(t)$ of a charged particle can be solved for as a function of time t by means of numerical integration of the ordinary differential equation (ODE) (1). It is noteworthy that due to the magnetic term in (1) a charged particle experiences an azimuthal force even for axisymmetric electromagnetic fields with vanishing azimuthal components $E_\varphi = B_\varphi = 0$.

Equation (1) can be analyzed independently both for electrons ($q = -e$; $m = 1\ m_e$) and positive Ar^+ ions ($q = +e$; $m = 40$ u $\approx 72{,}915\ m_e$) with appropriate initial conditions: For the electrons initial positions can be assumed on the cathode surface $z(t = 0) = 0$ according to the primary mechanism of electron generation as a consequence of ion bombardment of the cathode surface, whereas Ar^+ ions are primarily generated in the plasma, i.e. $z(t = 0) > d$ with d as the sheath thickness. Inserting the electromagnetic fields given in the previous section into (1) it can be seen that electrons will swirl in more or less helical orbits above the cathode and about the axis of the magnetron, whereas the heavy Ar^+ ions are hard to magnetize [3]: Their response to the magnetic field is negligible and they almost travel along the electric field lines, i.e. normally onto the cathode surface without significant radial and azimuthal displacement. The different response can be explained by the difference in the gyro radii of electrons and ions: whereas for electrons the gyro radius is in the range of a few millimeters, it is in the range of meters for the ions under the given magnetic field.

From this it can be concluded that the radial and azimuthal position of an ionization event $e + Ar \rightarrow 2e + Ar^+$ taking place in the plasma will also determine the respective later position of the Ar^+ ion hitting the cathode and consequently the position of probable sputtering and secondary electron emission. Furthermore, it can be observed that most of the electron orbits are not ideally helical since their gyro radius of a few mm is of the same order of magnitude as the characteristic length of the electromagnetic field [3].

Depending on the initial position of electrons on the cathode surface one can see that some electrons are lost after a short time, whereas others are confined by the electric and magnetic fields, which allows them to perform a large number of ionizations [3]. Hence, one can conclude that a higher density of ionization events will take place within a well established confinement zone and consequently higher sputtering and target erosion rates will be found right below this region.

Equation (1) describes the motion of charged particles without consideration of inter-particle collisions such as the ones occurring between electrons, between electrons and ions as well as between electrons and neutrals. Electron-ion collisions [3] and electron-electron collisions [7] usually can be neglected for weakly ionized plasmas because of the low electron and ion density (as compared to the one of neutrals) leading to a rather low probability for these collisions to take place. Consequently, in a further step the discrete model is enhanced in order to account for collisions between electrons and neutrals, i.e. Ar atoms. This not only allows to resolve representative discrete positions of ionization events but also provides a mechanism for scattering of electrons out of the confinement after a finite time that otherwise would be indefinitely be trapped within this region [3], which would be physically questionable.

For the present model the following electron-neutral collisions as summarized in Table I are taken into account: elastic collisions, excitations, and ionizations, whereas others such as superelastic scattering, two-step, and penning ionizations are neglected [3]. Besides reducing the kinetic energy and velocity

magnitude of the impinging electron the collisions lead to scattering of the electrons, i.e. to a change of the velocity direction vector. The energy loss depends on the type of collision: for ionization of ground state Ar it amounts to 15.8 eV plus the kinetic energy of the secondary released electron; for excitation it depends on the level of energy to which the Ar atom is excited (11.5 - 15.8 eV); for elastic scattering it is proportional to the mass ratio of the electron and the Ar atom, which is $m_e/M \approx 1.37 \cdot 10^{-5}$. According to classical collision theory collisions are characterized by differential cross-sections $\mathrm{d}\sigma_c/\mathrm{d}\Omega$ [1] (in units of area/steradian) serving as a measure for the probability of a given collision to take place and to scatter the impinging electron to a particular angle α. The differential cross-sections are different for each type of collision and depend on the kinetic energy of the impinging electron. Integration of the differential cross-section yields the integrated cross-section σ_c (in units of area) serving as a measure for a particular collision to take place. From summation of the integrated cross-sections $\sigma_{c,i}$ over all $i = 1, \ldots, P$ types of collisions the total collision cross-section σ is obtained.

From the above analysis of collisionless orbits of charged particles it can be concluded that it is sufficient to know the ionization positions in order to determine the sputtering and erosion locations. Hence, this allows to solely trace the electrons' orbits based on (1) with considering the collisions as discontinuities in the velocity vector **v**. To this end, within the model collision events are triggered at random time instants for all electrons under consideration rather than modeling a "physical" collision between an electron and a neutral. Collisions are triggered by comparing random numbers – sampled for all electrons for each time step used for numerical integration of (1) – to the probability per time step of a collision to occur. The latter is continuously computed from the total cross-section of the electron based on its kinetic energy. If a collision is found to take place, the collision type is determined using another random number compared to the relative probability of each collision type. The colliding electron's velocity vector **v** in equation (1) is then reinitialized according to the energy loss corresponding to the particular type of collision and scattering angle α. The latter is determined from a third random number that is compared to the relative probability for a particular angle based on the differential cross-section $\mathrm{d}\sigma_c/\mathrm{d}\Omega$. The latter are taken as the ones for elastic scattering given in [8] and are assumed to be approximately valid in a relative sense for all three types of collisions [3]. Individual integrated cross-sections σ_c for the considered collisions are taken from [9]. Energy losses due to the inelastic collisions are assumed to be constant and taken as the respective threshold energies (see Table I). If a particular electron undergoes an ionization collision, its current position representing the spatial ionization location is stored and used to update statistical quantities such as the corresponding mean value and standard deviation.

Table I: Types of collisions considered within the discrete electron model

type of collision	formula	threshold energy [eV]
elastic scattering	$e + Ar \rightarrow e + Ar$	0
excitation	$e + Ar \rightarrow e + Ar^*$	11.5
ionization	$e + Ar \rightarrow 2e + Ar^+$	15.8

Implementation

The presented model is implemented in spirit of the concepts of *Monte Carlo* codes using the scientific computation environment *Comsol Multiphysics* [4] which allows to model the entire problem within a single framework: using its finite element capabilities the magnetic field and flux density **B** are solved for using a discretization of the magnetostatic problem in an axisymmetric domain within a first analysis step (see also Fig. 3), whereas the electric field **E** is prescribed according to the improved *Child*'s law as a parameterized analytical function. Equation of motion (1) is implemented using the capabilities of the software in solving ODEs providing different time stepping schemes. This way, the trajectories of an arbitrary large set of m_e electrons are computed over a series of an arbitrary number of transient runs m_{run}. Time stepping for each run is achieved using an implicit BDF time stepping scheme [4] with a maximum step size of 50 ps over a maximum period of 2.5 μs [3]. Electrons leaving the computational domain and electrons of very low kinetic energy are set inactive with their orbits not further traced.

For each run electrons are released from the cathode surface in a random fashion accounting for the probability of the radial position of ion bombardment and secondary electron emission. To this end, a probability density function for the radial coordinate of electron emission is defined, which is constantly updated according to the positions of the ionizations having occurred so far. The probability density function has to be initialized for the first run (either based on an initial guess from *a priori* knowledge or simply based on a uniform distribution function) and considers the ionization statistics from all preceding runs for each of the subsequent ones. Experience from application of the model shows that the statistical measures converge quite fast such that an initial guess of particular quality is not required.

The present implementation is very flexible in terms of the choice for the size m_e of the electron set and the number of consecutive runs m_{run}. In practice, choosing appropriate values becomes a trade-off between desired accuracy and required run-time. Setting $m_e = 1$ and m_{run} to an arbitrary integer in fact yields the scheme adopted in [3] tracing one electron at a time. Experience from application of the model, however, reveals that the cost for the time stepping procedure scales less than linearly in the number of electrons per run. Hence, it appears to be more economic – still at the same accuracy – to account for a significantly larger number of electrons used in a reduced number of consecutive runs. For example, for the axisymmetric magnetron under consideration it appears practical to assume $m_e = 100$ and $5 \leq m_{run} \leq 10$.

Results

Exemplary orbits of ten electrons (for the sake of clarity sampled from the considered set of $m_e = 100$ electrons) are shown in Fig. 4 projected onto the *rz*-plane (top) and $r\varphi$-plane (bottom). Orbits are given over an initial period of 0.1 μs for the first three runs $m_{run} = 1…3$ (from left to right). For the first run (left) uniform probability density for secondary electron emission over the radial coordinate of the cathode surface is assumed, whereas an updated function is used for the consecutive runs. Initial positions of electrons are indicated by square symbols, whereas the current positions (or the positions of rest of inactive electrons) are given by circles. It is clearly seen that electron emission density converges rapidly reducing the probability for emission of unconfined electrons: Within the first run (left) 50% of the electrons have left the computational domain after just 0.1 μs since being unconfined by the

electromagnetic fields, whereas within the third run (right) all electrons are still active. Nonetheless, they will be scattered out of the confinement due to collisions during further run-time, thus, gradually reducing the number of active electrons. Some kinks in electron trajectories (best seen in their $r\varphi$-plane projections in Fig. 4) indicate first collision events accompanied by obvious scattering. For the seventh run (not shown) app. 30% of the electrons are still active after a period of 2.5 μs, however, only about 7% of the initial electron population is capable to perform ionizations having a kinetic energy greater than the ionization threshold energy of 15.8 eV.

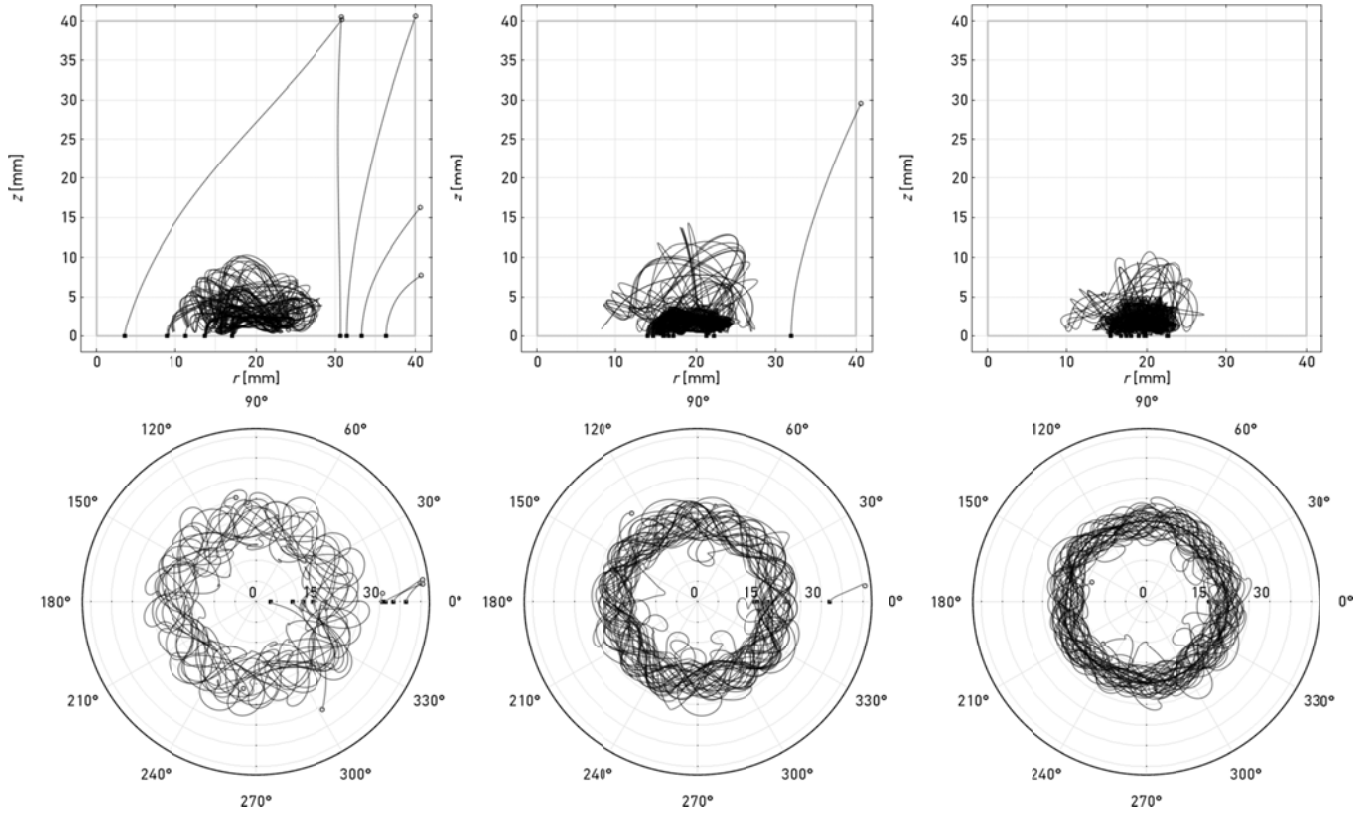

Figure 4: Electron orbits for ten randomly selected electrons over an initial period of 0.1 μs for the first three runs (from left to right) in rz-plane (top) and $r\varphi$-plane (bottom) with initial and current positions (or positions of rest of inactive electrons) indicated by square and circle symbols, respectively.

Ionization positions are stored in a cumulative fashion over all runs and classified in a two-dimensional histogram domain in the rz-plane and in integrated fashion over the z- and r-direction in one-dimensional histograms along the radial coordinate of the cathode surface and the magnetron axis, respectively. For the histograms bins of 1 mm width are used.

Fig. 5a depicts the cumulative number of ionization events in the rz-plane normalized using the maximum value as obtained after seven runs each with 100 electrons. The maximum ionization density is found in the interval r = [19, 20] mm, i.e. at the position of vanishing axial component of the magnetic flux density $B_z = 0$ (cf. Fig. 3b), and z = [2, 3] mm, i.e. right above the sheath, where electrons exhibit maximum kinetic energy after been accelerated through the sheath. In Figs. 5b and 5c respective normalized histograms for the ionization locations along the r- and z-axis are given, again revealing the location of maximum ionization density. The normalized radial ionization density profile exhibits its mean value at r = 19.2 mm with a standard deviation of ±3.6 mm after seven runs. It should be noted that the

statistical measures converge quite fast with the ones obtained after the very first run found within ±0.02 mm tolerance.

As already mentioned, the radial ionization density profile can be considered as a qualitative representation for target erosion. Thus, it can be concluded that maximum target erosion will take place at $r \approx 19$ mm, which correlates well to the shape of the magnetic field shown in Fig. 3b and the respective empirical observation [2] mentioned above.

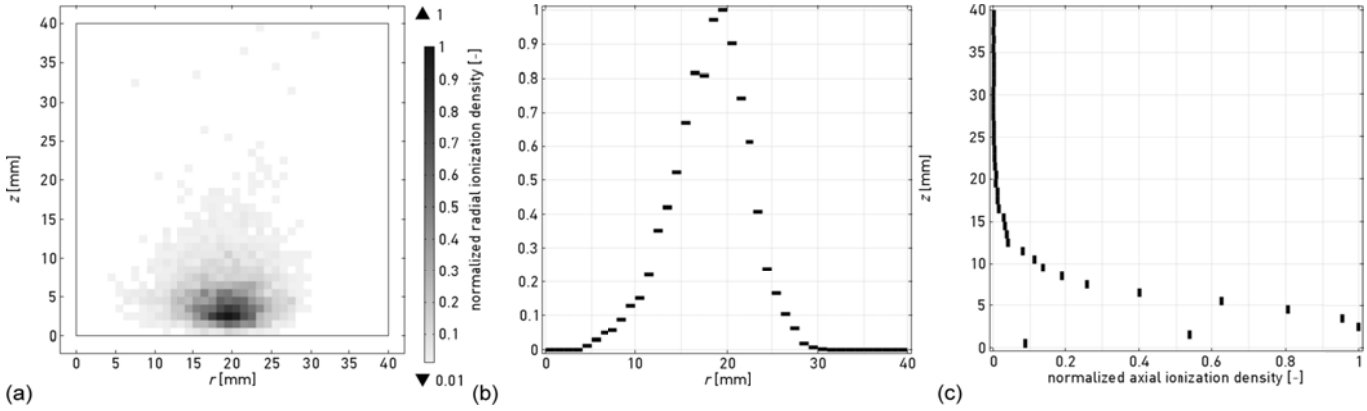

Figure 5: Results obtained from model with discrete collisions: normalized ionization density (a) in *rz*-plane, (b) along radial coordinate over cathode surface, (c) along magnetron axis.

The results shown in Fig. 5 perfectly agree to the numerical results given in [3], where also an experimentally measured erosion profile is given for the particular magnetron.

Modified Discrete Model

The model shown in the previous section mostly follows the approach proposed by *Sheridan* and coworkers [3] and the present implementation within *Comsol Multiphysics* [4] is reliable as can be seen from the perfect agreement of the results. Nonetheless, even though this implementation is already tuned – by means of appropriate choices for the size of the electron population and the number of runs – it still suffers from the disadvantage of being computationally rather expensive in order to obtain the desired accuracy. Though this is of minor importance for studying the mechanisms in a given setting, it makes the present approach less attractive for studying design variations of the magnetron, for instance, in order to optimize target utilization.

Hence, within the following an alternative approach is proposed which allows for shorter run times and its application to parametric studies. To this end, the model shown in the previous section is modified in that collisions are not considered as discrete events taking place at random time instants and represented by reinitializing the electron's velocity vector **v**. Instead they are accounted for by a frictional force continuously acting on the electron with its magnitude expressed in terms of the total collision cross-section. To this end, equation (1) is modified as

$$\mathbf{a} = q/m \cdot (\mathbf{E} + \mathbf{v} \times \mathbf{B}) - \nu\,\mathbf{v} \qquad (2)$$

with the collision frequency ν expressed in terms of the neutral number density N and the total collision cross-section $\sigma = f(|\mathbf{v}|)$ as

$$\nu = N\,\sigma\,|\mathbf{v}|. \qquad (3)$$

Note that the frictional term in (2) acts parallel and in opposite direction to the current velocity vector of the electron. Hence, it tends to reduce the electron's velocity but does not allow to change its direction of motion. Consequently, scattering of electrons cannot be considered. This, however, is only of minor concern since equation (2) should be interpreted as an average trajectory of an infinite number of electrons having the same initial conditions – in particular being emitted at the same radial position from the cathode surface – rather than representing the orbit of a single electron. Since each of these electrons will experience collisions at different time instants and positions along its trajectory, equation (2) can be considered to describe an envelope over the infinite number of electrons.

Solving for equation (2) rather than for (1) together with discrete collisions events exhibits the advantage that the time stepping procedure does not have to be stopped and re-initialization of the ODE to be performed from time to time. Furthermore, continuous sampling of random numbers and their comparison to probabilities becomes obsolete. This offers significant advantages in terms of computational performance and still guarantees acceptable accuracy. However, with collisions not explicitly resolved, locations of ionizations and ion bombardment on the cathode surface cannot be directly determined anymore. As a remedy rate equations are solved onto the same discretization used for ionization counting for the model with discrete collisions. Thus, histogram classes are now used as spatial finite element discretizations (with discontinuous finite elements using a single integration point) where relative probabilities for ionization events are integrated over all electrons currently found within a particular element. This way, probabilities for ionization within a particular spatial interval are determined which over the entire domain can be interpreted as ionization density distributions.

Application of the modified model shows that most of the qualitative features of the radial and axial ionization profiles are resolved in almost the same fashion as by the model based on discrete collision events (Fig. 6). In particular, the mean value and standard deviation for the radial ionization positions are found to be 19.2 ± 3.2 mm. Hence, the position of the maximum ionization density and erosion rate are accurately resolved by the model, however, the radial extend is somewhat underestimated as indicated by the slightly lower standard deviation as can be seen from the somewhat narrower profile in Fig. 6a. This can be explained by the inability of the modified model to resolve scattering of electrons which otherwise allows electrons to step-by-step leave their confinement and perform at least some ionizations outside the latter. Despite of this circumstance the modified model yields reasonable results that can be obtained within a fraction of the run time required for the model based on discrete collision events. Thus, the model appears to be a suitable means to quickly study design modifications of a magnetron, for instance, in order to perform a required optimization. If an optimal configuration is found using the modified model, the refined model based on discrete collision events can then be applied for verification purposes.

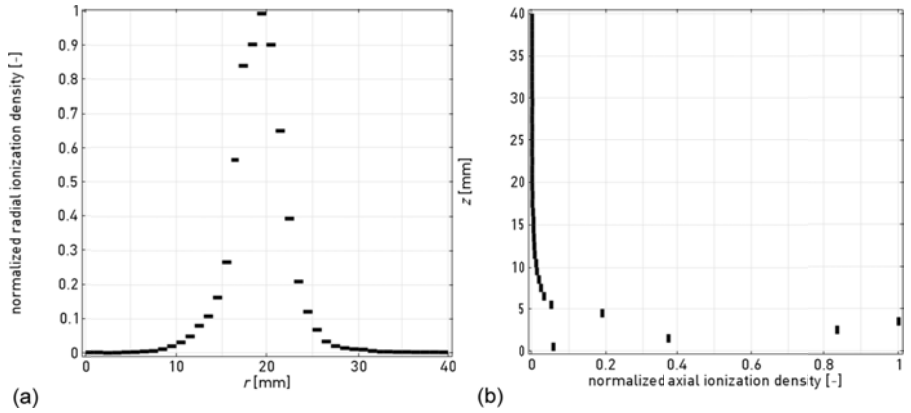

Figure 6: Results obtained from modified model: normalized ionization density (a) along radial coordinate over cathode surface, (b) along magnetron axis.

This would require only a single run for a set of electrons with initial conditions for the electron emission probability function as obtained from the modified model.

Summary

A numerical model for studying the mechanisms within magnetically enhanced direct current (DC) discharges is implemented. Such discharges are employed in planar magnetrons widely used in industry for sputtering and deposition of metals – such as the refractory metals molybdenum or tungsten – onto various substrates. Though allowing to be operated at relatively low pressure – this way reducing spurious (re-)depositions on the cathode and other walls – sputtering processes in magnetrons are characterized by rather non-uniform target erosion and low target utilization.

The model implemented in the present work aims at studying target erosion and at increasing target utilization. To this end, a model similar to the one proposed by *Sheridan* and coworkers [3] and formulated in the spirit of a discrete *Monte Carlo* approach is implemented within a commercial scientific computation environment. The model resolves trajectories of high energetic electrons emitted at the cathode surface with collisions taking place at discrete random time-instants. Locations of ionization collisions are stored and considered to represent the locations of ion bombardment, target erosion, and secondary electron emission after projection onto the cathode surface along the electric field lines.

For verification purposes the present implementation is tested using the reference problem studied by *Sheridan* and coworkers [3]. Perfect agreement with the reference results is achieved. Since despite of some tuning being computationally rather expensive the model is modified in that collisions are considered by means of a frictional force – acting on the electrons and accounting for the integrated cross-sections as a function of kinetic energy – rather than in discrete manner. This way, performance of the model is significantly increased still at acceptable accuracy. Though the proposed modification represents a simplification it appears to be well suited for studying design modifications of magnetrons.

References

1. M.A. Lieberman and A.J. Lichtenberg, *Principles of Plasma Discharges and Materials Processing*, Second Edition, John Wiley & Sons Inc., Hoboken (NJ), (2005)

2. Q.H. Fan, L.Q. Zhou and J.J. Gracio, *J. Phys. D: Appl. Phys.* **36**, 244-251, (2003)
3. T.E. Sheridan, M.J. Goeckner and J. Goree, *J. Vac. Sci. Technol.* **A8** [1], 30-37, (1990)
4. COMSOL, *COMSOL Multiphysics User's Guide Version 4.3a,* (2012)
5. T.E. Sheridan and J. Goree, *J. Vac. Sci. Technol.* **A7** [3], 1014-1018, (1989)
6. T.E. Sheridan and J.A. Goree, *IEEE Trans. Plasma Sci.* **17** [6], 884-888, (1989)
7. S.M. Rossnagel, J.J. Cuomo and W.D. Westwood (eds.*), Handbook of Plasma Processing Technology – Fundamentals, Etching, Deposition, and Surface Interactions*, Noyes Publications, Park Ridge (NJ), (1990)
8. S.N. Nahar and J.M. Wadehra, *Phys. Rev. A* **35** [5], 2051-2064, (1987)
9. http://www.lxcat.laplace.univ-tlse.fr/cross_sec_download.php (visited 02/2013)